Applied Catalysis A: General 450 (2013) 160–168

Contents lists available at SciVerse ScienceDirect

Applied Catalysis A: General

journal homepage: www.elsevier.com/locate/apcata

Effect of $(Zn(OH)_2)_3(ZnSO_4)(H_2O)_5$ on the performance of Ru–Zn catalyst for benzene selective hydrogenation to cyclohexene

Hai-jie Sun[a], Hong-xia Wang[a], Hou-bing Jiang[a], Shuai-hui Li[a], Shou-chang Liu[a], Zhong-yi Liu[a,*], Xue-min Yuan[b], Ke-jian Yang[b]

[a] Department of Chemistry, Zhengzhou University, Zhengzhou 450001, Henan, PR China
[b] China Tianchen Engineering Corporation, Tianjin 300400, PR China

ARTICLE INFO

Article history:
Received 5 August 2012
Received in revised form
25 September 2012
Accepted 10 October 2012
Available online 8 November 2012

Keywords:
Benzene
Selective hydrogenation
Cyclohexene
Ruthenium
Zinc

ABSTRACT

A series of Ru–Zn catalysts with different Zn contents were prepared by co-precipitation. The catalysts were characterized by X-ray diffraction (XRD), X-ray photoelectron spectroscopy (XPS), Auger electron spectroscopy (AES) – Ar^+ sputter, transmission electron micrographs (TEM)–energy dispersion scanning (EDS) and temperature-programmed reduction (TPR). The performances of the catalysts for benzene selective hydrogenation to cyclohexene were investigated in the presence of 0.6 mol/L of $ZnSO_4$. The results showed that the Ru and Zn in Ru–Zn catalyst were in metallic Ru and ZnO respectively and the ZnO was rich on the surface. The ZnO alone could not improve the selectivity to cyclohexene of Ru–Zn catalyst. However, the ZnO on the surface could react with $ZnSO_4$ to form a $(Zn(OH)_2)_3(ZnSO_4)(H_2O)_5$ salt. The $(Zn(OH)_2)_3(ZnSO_4)(H_2O)_5$ salt chemisorbed played a key role in improving the selectivity to cyclohexene of Ru–Zn catalysts. After Ru–Zn(8.6%) catalyst was pretreated 22 h in $ZnSO_4$ solution at 140 °C and 5 MPa H_2, a cyclohexene selectivity of 81.4% at a benzene conversion of 54.0% was achieved at 10 min and a maximum cyclohexene yield of 58.9% was reached. Moreover, the activity was stable above 50% and the cyclohexene selectivity and yield were steadily above 76% and 40% on this catalyst in the first six recycles, respectively.

1. Introduction

There has been a growing interest in using heterogeneous catalysts for the selective hydrogenation of benzene to cyclohexene, a greener intermediate feedstock than cyclohexane for producing nylons and fine chemicals [1–6]. However, it is thermodynamically difficult to obtain cyclohexene in high selectivity. Therefore, it has been long time that only cyclohexane was obtained during the hydrogenation of benzene [7]. In 1989, the Asahi Chemical Industry Co. industrialized the process for producing cyclohexene from the partial hydrogenation of benzene employing an unsupported Ru–Zn catalyst, and a cyclohexene yield of 32% at a benzene conversion of 40% was obtained [8,9]. However, the yield of cyclohexene is still relatively low. Therefore, it is necessary to study catalyst preparation and modification in order to increase the yield of cyclohexene.

Some additives, which are directly put into the reaction system together with the catalyst and sometimes are called co-catalyst [8] and reaction modifier [10], can greatly improve the selectivity to cyclohexene. Generally, there are two kinds of additives: organic [4,11–13] and inorganic [8,14,15]. Effective organic additives should contain a polar group such as hydroxyl or amine group. However when using these organic additives the selectivity to cyclohexene never exceeded 40%. Inorganic additives such as Zn, Fe, Co, Ni, Cd, Ga, and In salts are more effective than organic additives [14]. Among them, $ZnSO_4$ has been regarded as the best additives. Struijk et al. [14] used XPS to characterize Ru catalyst after hydrogenation in the presence of $ZnSO_4$ under the reaction conditions of 423 K and 5.0 MPa of H_2, and found the majority of chemisorbed Zn is present as Zn^{2+}. They suggested that the chemisorbed Zn^{2+} could enhance the hydrophilicity of Ru catalyst and selectively cover the most reactive sites, which improved selectivity to cyclohexene of Ru catalyst. Based on these, they specially pointed out the salts as effective additives should have a high absorbability on ruthenium surface and a difficult reduction ability under the reaction conditions.

The promoters also have great impacts on the yield of cyclohexene. It was reported that K [16], Fe [17–19], Co [13,20], Ce [21], Ba [22], La [15,23,24] and Zn [4,8,25–29] as a promoter or co-promoters to modify the ruthenium by co-precipitation or co-impregnation or other methods were beneficial for the increase of the selectivity to cyclohexene. Among them, Zn has been considered to be the best promoter [4,8]. Wang et al. [26] and He et al. [28] prepared Ru–Zn/ZrO_2 catalysts using hydrogen reduction of

* Corresponding author. Tel.: +86 371 67783384.
E-mail address: liuzhongyi@zzu.edu.cn (Z.-y. Liu).

0926-860X/$ – see front matter © 2012 Elsevier B.V. All rights reserved.
http://dx.doi.org/10.1016/j.apcata.2012.10.016

coprecipitation product of ruthenium trichloride and zirconium oxychloride in a $ZnSO_4$ solution under the reaction conditions of 423 K and 453 K as well as H_2 pressure of 4.28 MPa and 5.0 MPa respectively. The catalysts were characterized by XPS, and it was found that the BE of Zn $2p_{3/2}$ of the Zn in the catalyst was close to that of metallic Zn. So they thought the chemisorbed Zn^{2+} could be reduced by H atoms which spilled from metallic ruthenium surface [26,28]. Wang et al. [26] suggested that the metallic Zn could irreversibly occupy the most reactive sites unfavorable for benzene selective hydrogenation. Yuan et al. [27] indicated that the presence of Zn atoms on the surface of the Ru–Zn alloy resulted in a direct decrease in sites for the chemisorption of cyclohexene but also a depressed adsorption capability of the neighboring surface Ru sites. Therefore, Ru-based catalyst modified by metallic Zn gave a high selectivity to cyclohexene. However, the binding energies (BEs) of metallic and oxidized Zn are very close and it is difficult to assess the oxidation state of zinc by XPS measurements [30].

As mentioned above, the $ZnSO_4$ as an additive could not be reduced. The Zn^{2+} as a promoter, however, could be reduced to metallic state under the similar condition. Obviously, there is a severe contradiction. Moreover, the roles of the promoter and the additive were described in separate and the interactions between them were ignored in all published documents [15,21]. Motivated by these problems, a series of Ru–Zn catalysts with different Zn contents were prepared. In order to discern the oxidation state of Zn in Ru–Zn catalysts AES-Ar^+ sputtering were employed since the Auger shift between Zn^{2+} and Zn^0 is higher than 4.6 eV [31]. It is found that the Zn in Ru–Zn catalyst exists as ZnO which is rich on the surface. Only ZnO cannot improve the selectivity to cyclohexene of Ru–Zn catalyst. ZnO on the surface can react with the additive $ZnSO_4$ to form a insoluble $(Zn(OH)_2)_3(ZnSO_4)(H_2O)_5$ salt. The $(Zn(OH)_2)_3(ZnSO_4)(H_2O)_5$ salt plays a key role in improving the selectivity to cyclohexene of Ru–Zn catalysts and its modification effects are discussed.

2. Experimental

2.1. Catalyst preparation

Ru–Zn catalysts were prepared according to the procedure in the literature [32]. 9.75 g $RuCl_3{\cdot}H_2O$ and a desired amount of $ZnSO_4{\cdot}7H_2O$ were dissolved in 200 ml H_2O with agitation. To the stirred solution, 200 ml of a 20% NaOH solution was added instantaneously and the resulting mixture was agitated for an additional 4 h at 353 K. The mixture was left to stand and the black precipitate was washed three times with an aqueous solution of 5% NaOH after the supernatant had been removed by decantation. This black precipitate was dispersed in 400 ml of a 5% NaOH solution and charged into a 1 L autoclave lined the Teflon. Hydrogen was introduced into the autoclave to raise the total internal pressure to 5 MPa and the reduction was conducted at 423 K and at 800 r/min stirring rate for 3 h. The reaction mixture was cooled and the obtained black powder was washed three times with 5% NaOH, then with water until neutrality, subsequently vacuum-dried and the desired Ru–Zn catalysts were obtained. The catalyst was divided into two shares, one share was used for activity test and the other for catalyst characterization. This method ensured that the catalysts with different Zn contents had the same Ru contents (about 1.8 g Ru). The amounts of $ZnSO_4{\cdot}7H_2O$ were adjusted to give the catalyst with different Zn contents which were denoted as Ru–Zn(x) catalysts, where x denoted the weight percentage of Zn in the catalyst determined by atomic absorption spectrometry.

2.2. Catalyst characterization

N_2 physisorption (BET) was determined on a Quantachrome Nova 100e apparatus at 77 K. The sample was heated at 423 K under vacuum for 2 h before measurement. The pore size distribution was calculated from the desorption branch of the isotherm by the Barret–Joyner–Halenda (BJH) method. X-ray diffraction (XRD) patterns were acquired on a PANalytcal X'Pert PRO instrument using Cu Kα (λ = 1.541 Å) with scan range from 5° to 90° at a step of 0.03°. The atomic absorption spectroscopy (AAS) for determining the Zn content of the catalyst was performed on a Perkin Elmer AAnalyst 300 instrument, operating at λ = 213.9 nm and slit width = 0.20 nm. The Zn/Ru molar ratio was measured by X-ray fluorescence (XRF) on a Bruker S4 Pioneer instrument. Surface analysis of the catalysts was analyzed by X-ray photoelectron spectroscopy (XPS) on a PHI Quantera SXM instrument using a monochromatized Al Kα radiation (E_b = 1486.6 eV) at an energy resolution of 0.5 eV and at a base pressure of 3×10^{-8} Pa. The energy scale was calibrated and corrected for charging using the C1s (284.8 eV) line as the binding energy reference. Auger electron spectroscopy (AES) and sputter profiles were taken on a ULVAC PHI-700 Nano-canning Auger system with on-axis scanning argon ion gun and CMA energy analyzer. The energy resolution ratio was 0.1%. The background pressure of analysis room was less than 5.2×10^{-7} Pa. The standard sample was SiO_2/Si. The sputtering rate was 9 nm/min. Transmission electron micrographs (TEMs) and energy dispersion scanning (EDS) were observed on a JEOL JEM-2100 instrument using an accelerating voltage of 200 kV. Temperature-programmed reduction (TPR) measurements were carried out in a U-shaped quartz reactor, using a 5% H_2/He gas flow of 50 $cm^3\ min^{-1}$, a thermal conductivity detector (TCD) and about 10 mg of catalyst.

The electron density of benzene, cyclohexene and cyclohexane was calculated by Gaussian 09 program under the level of B3LYP/6-31g (d, p).

2.3. Activity testing

The selective hydrogenation of benzene was performed in a 1 L autoclave lined the hastelloy. The autoclave was charged with 280 ml of H_2O containing a share of Ru–Zn(x) catalyst, 49.2 g of $ZnSO_4{\cdot}7H_2O$ and 9.8 g of ZrO_2. Then heating commenced with H_2 pressure of 5 MPa and stirring rate of 800 r/min. 140 ml of benzene was fed and the stirring rate was elevated to 1400 r/min to exclude the diffusion effect when the temperature reached 423 K. A small amount of reaction mixture was sampled every 5 min and sent for gas chromatographic analysis with a FID detector, and the benzene conversion and cyclohexene selectivity were calculated. After the reaction the organic was removed, the solid sample was washed with distilled water until no Zn^{2+} and then was vacuum-dried for characterization. The sample after reaction corresponding to Ru–Zn(x) catalysts was denoted as Ru–Zn(x)AH, where AH stood for After hydrogenation.

The effect of the pretreatment and the recyclability of Ru–Zn(8.6%) catalyst were investigated according to the following procedures. A share of Ru–Zn(8.6%) catalyst was pretreated for 22 h in the presence of 280 ml H_2O containing 49.2 g of $ZnSO_4{\cdot}7H_2O$ and 9.8 g of ZrO_2 at 413 K and with a H_2 pressure of 5.0 MPa as well as a stirring rate of 800 r/min. Then the temperature was raised to 423 K and hydrogenation was performed according to the above hydrogenation procedures. At the end of the reaction, the autoclave was cooled down and the organic phase was separated. The slurry containing the mixture of the catalyst and ZrO_2 was recycled in accordance with the above hydrogenation procedures without the pretreatment.

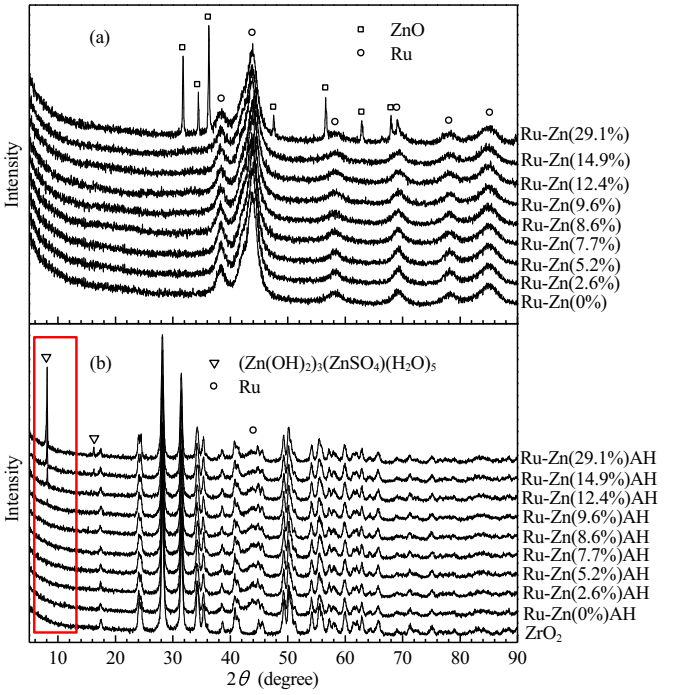

Fig. 1. XRD patterns of (a) Ru–Zn(x) catalysts and (b) Ru–Zn(x)AH.

3. Results and discussion

3.1. Structural and electronic properties

BET surface area, pore volume and pore diameter of Ru–Zn(x) catalysts are listed in Table 1. It can be seen that BET surface area decreases, and pore volume and average pore diameter increase with Zn content generally. Combined with TEM results, the formation of big ZnO particle on the surface of Ru–Zn(x) catalysts might be responsible for this. Table S1 shows the BET surface area, pore volume and pore diameter of Ru–Zn(x)AH. It is found the BET surface area, pore volume and pore diameter of Ru–Zn(x)AH are bigger than that of ZrO_2. This is because Ru–Zn(x)AH are composed by a fine mechanical mixture of Ru–Zn(x) catalyst and ZrO_2, as confirmed by the TEM results. The BET surface area, pore volume and pore diameter of Ru–Zn(x)AH changes little with the Zn contents. This probably relates to the weight ratio of ZrO_2 to the catalyst (5:1).

XRD patterns of Ru–Zn(x) catalysts (Fig. 1(a)) show that the diffraction peaks observed at 2θ of 38.4°, 44.0°, 58.3°, 69.4°, 78.4° and 84.7° are assigned to the metallic Ru phase (JCPDS: 01-070-0274). Evaluation of the Ru crystallite size from XRD using the Scherrer formula (Table 1) indicates Zn species addition has little influence on the Ru crystallite sizes of Ru–Zn(x) catalysts. However, Hu et al. [25] prepared a series of Ru–Zn/SiO_2 catalysts with various Zn contents by an incipient wetness co-impregnation method and found that increasing Zn species addition increased the Ru crystallite size. Obviously, this difference was caused by different catalyst preparation methods. Seven new diffraction peaks of Ru–Zn(29.1%) catalyst at 2θ of 31.8°, 34.4°, 36.3°, 47.5°, 56.6°, 62.9° and 68.0° are ascribed to the hexagonal phases of ZnO (JCPDS: 01-070-2551), indicating the existence of ZnO in the catalyst. This implies that at least a part of Zn in Ru–Zn(x) catalysts exists as ZnO.

The comparison of the diffraction peaks of ZrO_2 and Ru–Zn(x)AH in Fig. 1(b) shows all the diffraction peaks of Ru–Zn(x)AH are attributed to the monoclinic phase of ZrO_2 (JCPDS: 00-024-1165) except for the reflections at 2θ of 8.1°, 16.2° and 44.0°. The wide and weak diffraction peaks at 2θ of 44° of Ru–Zn(x)AH correspond to the metallic Ru phase (JCPDS: 01-070-0274), indicating the small crystallite sizes of Ru. Two new diffraction peaks at 2θ of 8.1° and 16.2° belong to the phase of $(Zn(OH)_2)_3(ZnSO_4)(H_2O)_5$ (JCPDS: 01-078-0246). This reveals that the ZnO on catalyst surface reacted with the additive $ZnSO_4$ to form a insoluble $(Zn(OH)_2)_3(ZnSO_4)(H_2O)_5$ salt. The diffraction peaks at 8.1° appear and gradually increase with Zn content, indicating the increase of the $(Zn(OH)_2)_3(ZnSO_4)(H_2O)_5$ content. Combined with the XPS and AES results below, it is concluded that the Zn on the surface of Ru–Zn(x)AH exists as the $(Zn(OH)_2)_3(ZnSO_4)(H_2O)_5$ salt. However, the diffractions of the $(Zn(OH)_2)_3(ZnSO_4)(H_2O)_5$ salt are not detected on Ru–Zn(x)AH until the Zn content was 9.6 wt%. This was because of the low amount of the $(Zn(OH)_2)_3(ZnSO_4)(H_2O)_5$ salt below beyond the detection limit of the XRD instrument when the Zn content was lower than 9.6 wt%.

Especially, it is the ZnO on the surface of Ru–Zn catalyst, not the ZnO in the bulk, that can react with the additive $ZnSO_4$ in the slurry to form $(Zn(OH)_2)_3(ZnSO_4)(H_2O)_5$ since it is very difficult for $ZnSO_4$ in the slurry to enter into the bulk of the catalyst.

The Zn $2p_{3/2}$ binding energy (BE) of Ru–Zn(8.6%) catalyst(Fig. 2(a)) is 1021.7 eV which is close to that of ZnO (1021.6 eV) [33]. Its Zn LMM kinetic energies (KEs) are both 986.0 eV at the sputtering time of 0 s and 30 s, and it slightly increases to 986.5 eV at the sputtering time of 1 min. However, these values are a little lower than that (987 eV) of the Zn(II) species in the PtZn/C catalyst [31] and that (988.1 eV) of the Zn(II) species in the calcined un-reduced Pr/Cr–ZnO catalyst [30]. Based on these, it is concluded that the Zn in the catalyst exists as ZnO and there is no clear proof in favor of that ZnO can be reduced by the spilled H atoms from the metallic Ru. The peak of Ru 3d is overlapped by the peak of C 1s, moreover, Ru 3d is sensitive to be influenced by reactant and product [14]. Therefore, Ru $3p_{3/2}$ is employed for discussion. The profile of Ru $3p_{3/2}$ (Fig. 2(f)) shows a shoulder, which is decomposed into two contributions. The one at 461.9 eV is assigned to metallic Ru [34], whereas the other corresponds to oxidized Ru in RuO_2 [35]. This indicates that a small part of Ru on the surface of the catalyst with the most activity can be oxidized to RuO_2 during the treatment of catalyst washing or vacuum drying.

The AES depth profiles of Ru–Zn(8.6%) catalyst (Fig. 2(d)) show the concentration of Ru increases, and the Zn concentration as well as the O concentration decreases with the sputtering time, indicating the enrichment of ZnO on catalyst surface. Moreover, the atom ratio of Zn to O is 0.93 on the top surface of the catalyst, indicating the oxidation of a small part of metallic Ru with the most activity, which is in accordance with the XPS results. This ratio increases gradually with the sputtering time and reaches 1 at the sputtering time of 1 min (the depth of 9 nm), indicating that the content of RuO_2 decreases with the sputtering time and the bulk phase is composed of the metallic Ru and ZnO.

The Zn $2p_{3/2}$ BE of Ru–Zn(8.6%)AH (Fig. 2 (b)) is 0.7 eV higher than that for the Ru–Zn(8.6%) catalyst, while the chemical shift of metallic Zn relative to the Zn in ZnO is about 0.5 eV. Moreover, the Zn LMM KE (983.6 eV) of Ru–Zn(8.6%)AH (Fig. 2(e)) is 2.9 eV lower than that (986.5 eV) of Ru–Zn(8.6%) catalyst. All of these indicate that a new Zn(II) species, which is the $(Zn(OH)_2)_3(ZnSO_4)(H_2O)_5$ salt as confirmed by XRD, is formed during the hydrogenation process. And the Zn(II) species are electron-deficient.

Unfortunately, the peak of Ru $3p_{3/2}$ for Ru–Zn(8.6%)AH (Fig. 2(g)) becomes too dispersive to discriminate between the metallic Ru and RuO_2 due to the dispersion of ZrO_2. However, the peak of Ru $3p_{3/2}$ becomes complex, indicating the variation of atomic environment for Ru due to the formation of the $(Zn(OH)_2)_3(ZnSO_4)(H_2O)_5$ salt on the surface of catalyst. For this reason, it is difficult to directly judge whether the Zn(II) species donated some electrons to metallic Ru or sulfate since the sulfate is more effective than Ru in drawing electrons. However, the composition of Zn(II) species

Table 1
Physical properties and crystallite size of the Ru–Zn(*x*) catalysts.

Sample	BET surface area (m^2/g), SSA	Pore volume (cm^3/g)	Average pore diameter (nm)	Crystallite size (nm)[a]
Ru–Zn(0%)	88	0.18	4.1	4.1
Ru–Zn(2.6%)	77	0.18	4.8	4.3
Ru–Zn(5.2%)	67	0.15	4.6	3.8
Ru–Zn(7.7%)	74	0.17	4.5	3.7
Ru–Zn(8.6%)	77	0.16	4.0	3.9
Ru–Zn(9.6%)	55	0.15	5.3	4.3
Ru–Zn(12.4%)	66	0.27	8.2	4.0
Ru–Zn(14.9%)	64	0.27	8.4	3.8
Ru–Zn(29.1%)	57	0.22	7.8	3.8

[a] Determined by XRD.

was measured by the XRF instrument and it is found that the molar ratios of Zn/Ru and S/Ru are 0.44 and 0.06 respectively. This suggests that the amount of sulfate is much lower that of Zn(II) species on the surface of Ru–Zn(8.6%)AH. Moreover, Struijk et al. [14] found that the BE of S 2p for Ru catalyst after hydrogenation in the presence of $ZnSO_4$ was 169.9 eV, which was higher than the standard value (169.2 eV for $ZnSO_4$) [36]. All of these indicates that the sulfate gets few electrons from the Zn(II) species. These

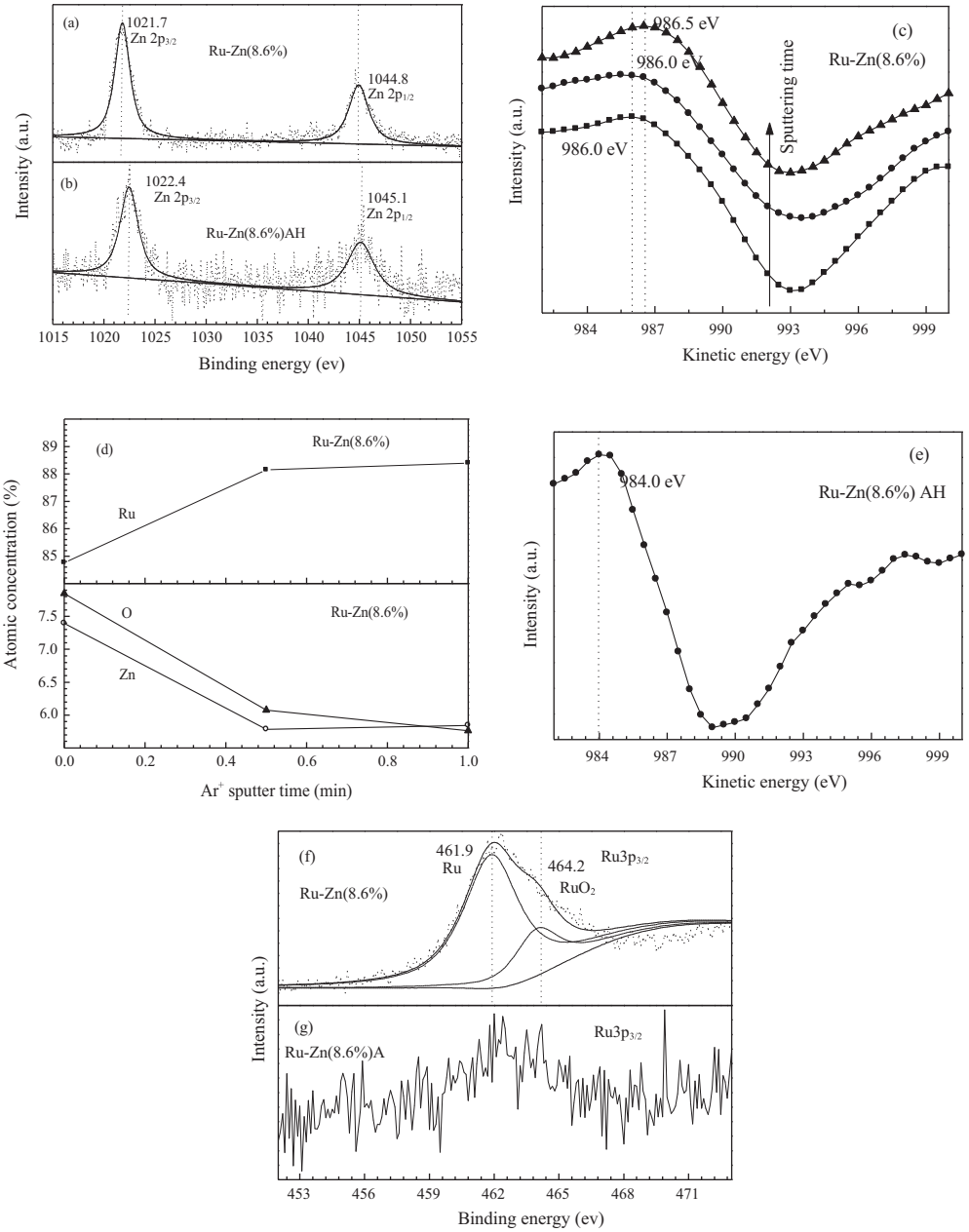

Fig. 2. (a) Zn 2p, (c) Zn LMM, (f) Ru $3p_{3/2}$ and (d) AES depth profiles of the Ru–Zn(8.6%) catalyst; (b) Zn 2p, (e) Zn LMM and (g) Ru $3p_{3/2}$ of the Ru–Zn(8.6%)AH sample.

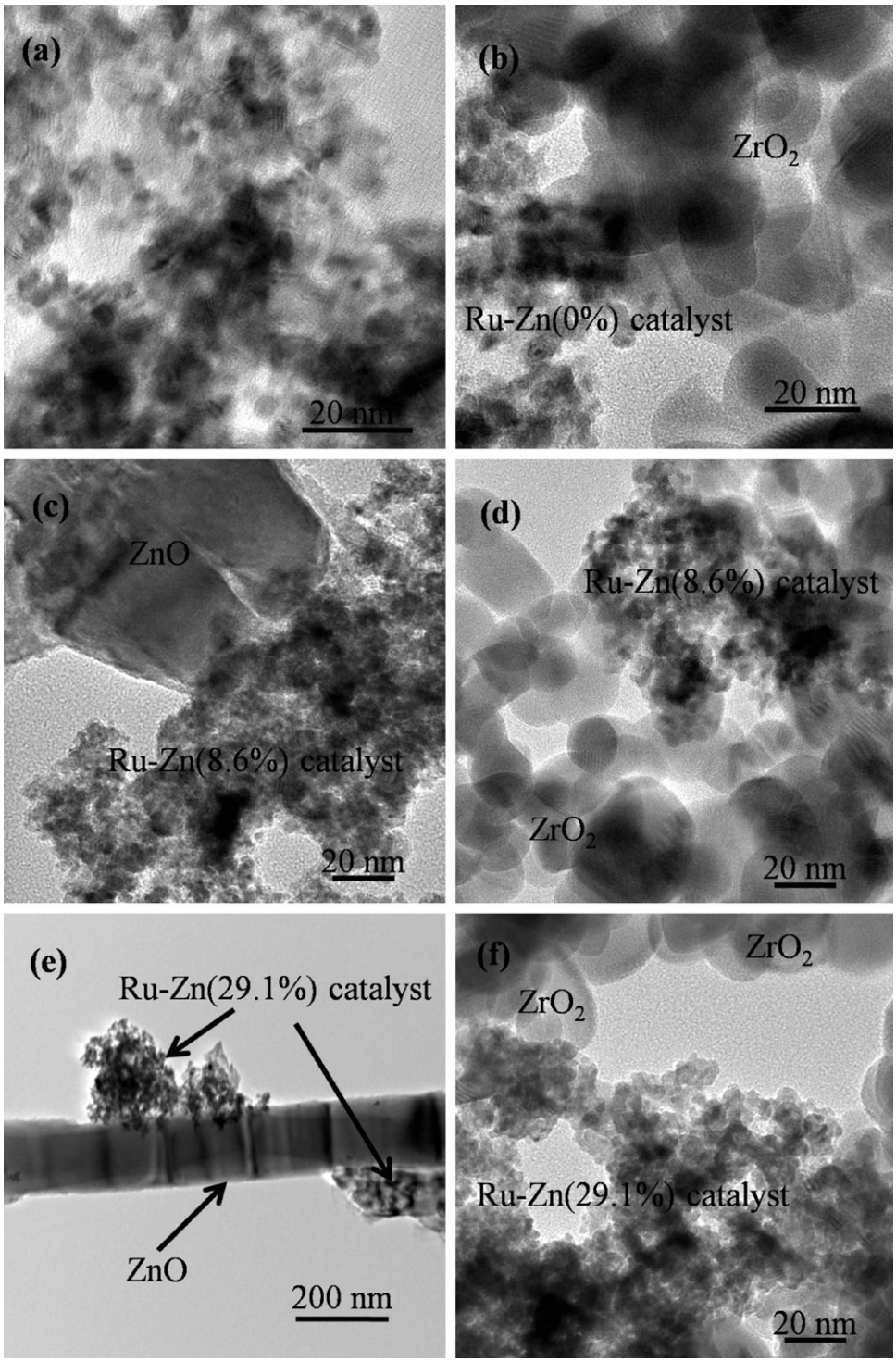

Fig. 3. TEM images of (a) Ru–Zn(0%) catalyst; (b) Ru–Zn(0%)AH; (c) Ru–Zn(8.6%) catalyst; (d) Ru–Zn(8.6%)AH; (e) Ru–Zn(29.1%) catalyst; (f) Ru–Zn(29.1%)AH.

prompt us to suggest that partial electrons might transfer from the Zn(II) species to the metallic Ru.

In addition, Table 2 shows that the pH values of the liquid phase after the reaction at room temperature are around 6.0 due to the hydrolysis of $ZnSO_4$. It is well known that increasing temperature favors the hydrolysis. This means that the acidity of liquid phase is much higher at the reaction temperature of 423 K due to the increase of hydrolysis degree of $ZnSO_4$. As we know, it is difficult for the metallic Zn to exist in the acid solution, which is consistent with no clear evidence of the presence of metallic Zn observed in the XPS and AES results.

TEM images in Fig. 3 show that the Ru crystallite sizes of Ru–Zn(0%) catalyst, Ru–Zn(8.6%) catalyst and Ru–Zn(29.1%) catalyst center on about 4 nm, which is consistent with the XRD results. It should be specially noted that the small particle in Fig. 3(c) and (d) is mainly composed of metallic Ru besides small amounts of Zn species. Thus they are generally denoted as Ru–Zn(8.6%) and Ru–Zn(29.1%) catalysts, respectively. A piece of thing is found on the surface of Ru–Zn(8.6%) catalyst in Fig. 3(c), which is confirmed

Table 2
Benzene conversion, cyclohexene selectivity and yield in 5 min as well as the maximum yield in 25 min over Ru–Zn(x) catalysts and pH value of liquid phase after the reaction.[a]

Catalyst	Conversion[b] (%)	Selectivity[b] (%)	Yield[b] (%)	Maximum yield[c] (%)	pH value[d]
Ru–Zn(0%)	57.9	38.2	22.1	23.1	5.7
Ru–Zn(2.6%)	68.1	47.2	32.1	32.1	5.8
Ru–Zn(5.2%)	54.4	69.5	37.8	48.0	5.9
Ru–Zn(7.7%)	50.5	71.1	35.9	47.4	5.9
Ru–Zn(8.6%)	46.0	76.2	35.1	50.9	6.1
Ru–Zn(9.6%)	26.4	84.1	22.2	50.4	5.9
Ru–Zn(12.4%)	20.7	86.0	17.8	49.8	6.1
Ru–Zn(14.9%)	13.1	87.5	11.5	34.2	5.8
Ru–Zn(29.1%)	6.8	90.4	6.2	19.0	6.0
Ru–Zn(0%)[e]	100	0	0	0	7.2
Ru–Zn(8.6%)[e]	86.7	1.9	1.6	1.6	7.3

[a] Reaction conditions: a share of catalyst, 49.2 g $ZnSO_4 \cdot 7H_2O$, 9.8 g ZrO_2, 280 ml H_2O, 5 MPa H_2, 423 K, stirring rate of 1400 r/min.
[b] Benzene conversion, cyclohexene selectivity and yield in 5 min.
[c] Maximum yield of cyclohexene in 25 min.
[d] pH value of liquid phase after the reaction at room temperature.
[e] In the absence of $ZnSO_4$.

to be ZnO by EDS. This also indicates that ZnO is rich on the surface and cannot be highly dispersed. Although the results of XPS, AES-Ar^+ and TEM all show the existence of ZnO, no ZnO phase is detected in XRD pattern of the Ru–Zn(8.6%) catalyst. This indicates that ZnO exists in the form of amorphous. Eo et al. [37] found that ZnO with heat treatment at 373–473 K for 60 min still showed an amorphous phase. Thus it is usual that no crystalline ZnO phases are detected when Zn content is lower than 29.1% since the catalyst reduction temperatures were only 423 K. A columnar ZnO (EDS confirmed) is displayed on the surface of Ru–Zn(29.1%) catalyst in Fig. 3(e), indicating its oriented growth under the catalyst preparation. This also accounts for the hexagonal phases of ZnO on Ru–Zn(29.1%) catalyst. Surprisingly, neither ZnO images nor the images of the $(Zn(OH)_2)_3(ZnSO_4)(H_2O)_5$ salt are detected on Ru–Zn(8.6%)AH in Fig. 3(d) and Ru–Zn(29.1%)AH in Fig. 3(f). This is probably due to the uniform dispersion of the $(Zn(OH)_2)_3(ZnSO_4)(H_2O)_5$ salt. Xie et al. [38] had confirmed that many salts could disperse spontaneously onto the surface of supports. More importantly, the different catalytic performances between Ru–Zn(8.6%) catalysts in the presence and in the absence of ZnSO4 (as described below) imply that only when the $(Zn(OH)_2)_3(ZnSO_4)(H_2O)_5$ salt uniformly disperses on Ru surface can the catalytic performance of Ru catalyst be significantly improved. Besides, the catalyst particles are separated and isolated by ZrO_2, indicating that ZrO_2 can reduce the chance of the collision of different catalyst particles under reaction condition of high agitation and suppress the agglomeration of the catalyst. Moreover, the added ZrO_2 also reduces catalyst adhesion to the metallic surface of the reactor. These are beneficial for the catalyst life [32].

The H_2-TPR profiles of Ru–Zn(x) catalysts (Fig. 4(a)) show peak shoulders between 300 K and 400 K. The shoulders are assigned to the reduction of RuO_2 to metallic Ru with the bid of XPS. Moreover, the process may experience the reduction Ru_2O_3 and/or RuO, thus the shoulders consist of two peaks or three peaks. Besides, the absence of any additional peaks indicates that the promoter ZnO cannot be reduced to metallic Zn within 500 K. Although bulk ZnO reduction is thermodynamically feasible, temperatures as high as 923 K are required. All the H_2-TPR profiles for Ru–Zn(x)AH (Fig. 4(b)) also appear peak shoulders between 300 K and 400 K which are also assigned to the step-by-step reduction of RuO_2 to metallic Ru. Obviously, the temperatures of complete reduction for all Ru–Zn(x)AH are lower than the reaction temperature of 423 K, indicating only the existence of metallic Ru under the conditions of 423 K and 5 MPa H_2.

3.2. Catalytic performance

The performances of Ru–Zn(x) catalysts with different Zn contents for selective hydrogenation of benzene to cyclohexene were investigated without the pretreatment. Benzene conversion, cyclohexene selectivity and yield in 5 min as well as the maximum yield in the reaction time over Ru–Zn(x) catalysts are summarized in Table 2. Fig. S1 gives benzene conversion and cyclohexene selectivity in 20 min. In Table 2 and Fig. S1, benzene conversion decreased and cyclohexene selectivity increased continuously with Zn content. Obviously, the increase of cyclohexene selectivity is at the expense of catalyst activity. Thus cyclohexene yield in 5 min and the maximum cyclohexene yield in reaction time are both first increased and then decreased with Zn content. A maximum cyclohexene yield of 50.9% was achieved on Ru–Zn(8.6%) catalyst.

The selectivity and the yield of cyclohexene reached 38.2% and 22.1% respectively at benzene conversion of 57.9% on Ru–Zn(0%) catalyst at 5 min in the presence of $ZnSO_4$. While in the absence of $ZnSO_4$ within only 5 min benzene was totally consumed on this catalyst. This indicates that the reaction of cyclohexene

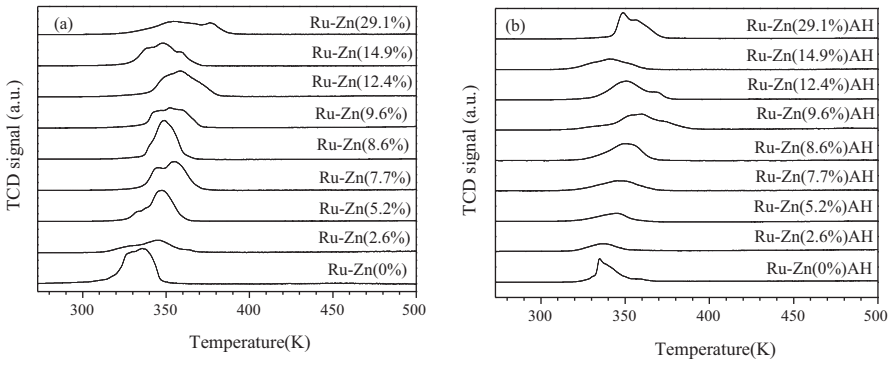

Fig. 4. H_2-TPR profiles of Ru–Zn(x) catalysts and Ru–Zn(x)AH.

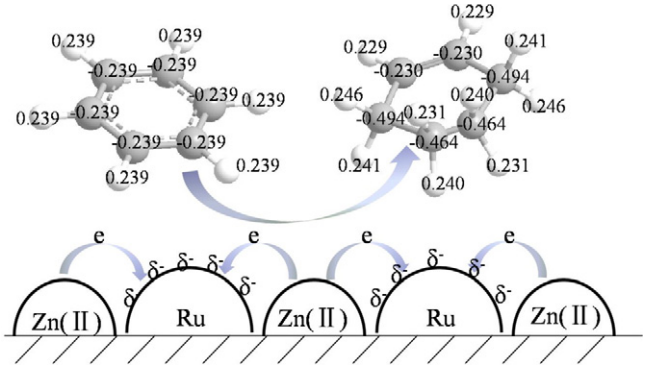

Fig. 5. Electronic interaction between Ru and Zn(II) species and electron cloud density of benzene and cyclohexene.

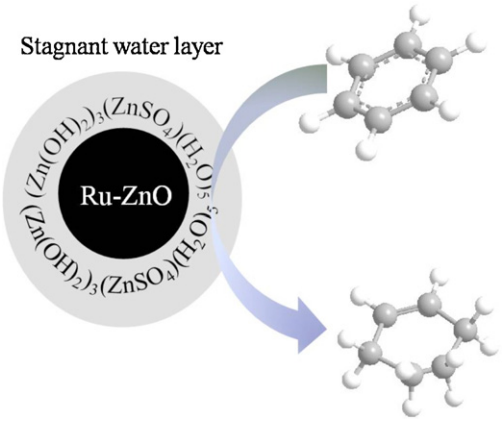

Fig. 6. Stagnant water layer formed by the chemisorbed $(Zn(OH)_2)_3(ZnSO_4)(H_2O)_5$ salt around Ru–Zn catalyst.

formation only happens on the surface of the Ru catalyst which can contact with $ZnSO_4$. For Ru–Zn(8.6%) catalyst, the conversion of benzene reached 86.7% within 5 min in the absence of $ZnSO_4$. The yield to cyclohexene was only 1.6% with the corresponding selectivity to cyclohexene of 1.9%. This implies that the promoter ZnO alone cannot enhance the selectivity to cyclohexene of Ru–Zn(8.6%) catalyst. However, this catalyst afforded a selectivity to cyclohexene of 76.2% and a cyclohexene yield of 35.1% with the corresponding benzene conversion of 46.1% at 5 min in the presence of $ZnSO_4$, indicating that the synergistic effect of ZnO and $ZnSO_4$ enhances the selectivity to cyclohexene of the catalyst. Namely, the $(Zn(OH)_2)_3(ZnSO_4)(H_2O)_5$ salt formed by the ZnO on the surface of the catalyst reacting with $ZnSO_4$ plays a key role in improving the selectivity to cyclohexene of the catalyst. Based on the catalyst characterization and the previous works, the roles of the $(Zn(OH)_2)_3(ZnSO_4)(H_2O)_5$ salt in improving the selectivity to cyclohexene of Ru–Zn catalyst can be attributed to the following reasons.

(1) It has been confirmed by XPS that the Zn(II) species of the $(Zn(OH)_2)_3(ZnSO_4)(H_2O)_5$ salt donates some electrons to Ru species and Ru is rich in electrons. The electron density of carbon atoms in benzene and cyclohexene is shown in Fig. 5. As can be seen, the electron densities of six carbon atoms of benzene are $-0.239e \times 6$, while that of cyclohexene are $-0.230e \times 2$, -0.494×2 and -0.464×2, respectively. This indicates that the electron densities of carbon atoms for cyclohexene are much higher than that for benzene. Thus the repulsive forces between the electrons around Ru and carbon atoms of cyclohexene are stronger than that between the electrons around Ru and carbon atoms of benzene, which is beneficial for the desorption of cyclohexene from the surface of the catalyst and improvement of the selectivity to cyclohexene. Meanwhile the activity of the catalyst decreases for the repulsive force between the electrons around Ru and carbon atoms of benzene.

(2) It has been demonstrated that the $(Zn(OH)_2)_3(ZnSO_4)(H_2O)_5$ salt can be uniformly dispersed on the active Ru sites (as confirmed by TEM). The Zn^{2+} of the chemisorbed $(Zn(OH)_2)_3(ZnSO_4)(H_2O)_5$ salt can selectively cover the most reactive sites of the catalyst, which can reduce the active sites for the chemisorption of cyclohexene and suppress the further hydrogenation of cyclohexene to cyclohexane. Therefore, increasing the content of the promoter increased the formation of the $(Zn(OH)_2)_3(ZnSO_4)(H_2O)_5$ salt, resulting in the decrease of activity and the increase of the selectivity to cyclohexene of Ru–Zn catalysts. Struijk et al. [14] suggested the salts which act as the effective additive should have enough absorbability on Ru to cover 50% Ru active sites.

$ZnSO_4$ also contains Zn^{2+}, however, it is a soluble salt and the Zn^{2+} chemisorbed on the surface of Ru active sites is very little. Therefore, $ZnSO_4$ can only improve the selectivity to cyclohexene to some extent. Although ZnO also has Zn^{2+}, it is difficult for it to be uniformly dispersed on Ru active sites (as confirmed by TEM). Thus Ru–Zn(8.6%) catalyst shows very little selectivity to cyclohexene in the absence of $ZnSO_4$.

(3) The $(Zn(OH)_2)_3(ZnSO_4)(H_2O)_5$ salt is abundant with crystal water. The crystal water can form a stable stagnant water layer around the Ru catalyst particles, as shown in Fig. 6. The diffusion rate of cyclohexene in water is very low due to its low solubility, indicating the low re-adsorption rate of cyclohexene through the stagnant water layer onto the surface of the catalyst [39]. This means it is hard for the desorbed cyclohexene to be re-adsorbed on the surface of the catalyst and hydrogenated to cyclohexane. Thus the selectivity to cyclohexene of the catalyst is improved. Meanwhile it is also difficult for the formed cyclohexene to diffuse through the stagnant water layer into the oil phase. However, the small cyclohexene droplets, mixed up with cyclohexane, can break through the stagnant water layer directly into the oil phase [39].

Above all, the $(Zn(OH)_2)_3(ZnSO_4)(H_2O)_5$ salt plays a key role in improving the selectivity to cyclohexene for Ru–Zn(9.9%) catalyst. The formation of the $(Zn(OH)_2)_3(ZnSO_4)(H_2O)_5$ salt is closely related to the ZnO content, especially its surface content, and the concentration of $ZnSO_4$. Thus the optimum Zn content has a close relationship with the concentration of the additive $ZnSO_4$. He et al. [28] also found this relationship, however, they could not give a good explanation for this based on the existence of Zn atoms.

The influence of pretreatment on the selectivity to cyclohexene of the Ru–Zn(8.6%) catalyst has also been investigated. Fig. 7(a) shows the pretreated catalyst afforded a maximum cyclohexene yield of 58.9%, which is among the best results reported so far [15,21]. Moreover, a selectivity to cyclohexene of 81.4% at a benzene conversion of 54.0% was achieved over the pretreated catalyst as shown in Fig. 7(b). The products of hydrogenation, benzene, cyclohexene and cyclohexane, were separated by solvent extraction due to their close boiling point. The higher the selectivity to cyclohexene is, the cheaper the cost of separation is. Thus the cyclohexene selectivity of more than 80% is requested by industry. Obviously, the performance of Ru–Zn(8.6%) catalyst meets this need.

XRF results reveal that the Zn/Ru and S/Ru molar ratios of Ru–Zn(8.6%) catalyst after the pretreatment slightly increase to 0.48 and 0.07 respectively, which is higher than those values (0.44 and 0.06) before the pretreatment. XRD (not shown) confirms that there are no other diffraction peaks detected besides the

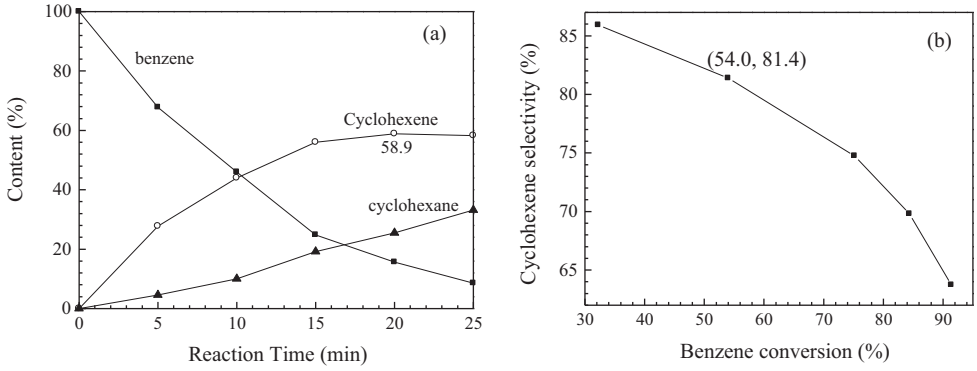

Fig. 7. (a) The course of the hydrogenation of benzene over the pretreated Ru–Zn(8.6%) catalyst and (b) cyclohexene selectivity as a function of benzene conversion over the pretreated catalyst. Pretreatment conditions: a share of catalyst, 280 ml H_2O, 49.2 g $ZnSO_4$, 5 MPa H_2, stirring rate of 800 r/min, temperature of 413 K. Reaction conditions: stirring rate of 1400 r/min, 140 ml benzene, and temperature of 423 K.

reflections of metallic Ru and ZrO_2. Struijk et al. [14] investigated the influence of the pretreatment on unsupported Ru catalysts and found that the metal cations chemisorbed on the catalyst surface improve the selectivity to cyclohexene and decrease the activity, which originate from corrosion of the stainless steel wall of the reactor. However, there is no Fe or other metallic elements detected after the pretreatment of the catalyst since our hydrogenation is performed in a hastelloy autoclave, which has a high resistance to acid. Milone et al. [40] carried out the pretreatment of Ru/γ-Al_2O_3 catalysts and suggested that the pretreatment gave a more reduced catalyst, which exhibited the higher selectivity to cyclohexene. However, TPR results have confirmed that the ruthenium oxide is completely reduced to metallic Ru under our hydrogenation conditions. Some of authors [5] also suggested hydrogen was preferentially adsorbed on the most active sites and benzene could only adsorbed on the moderately active sites, which benefited for the activation of benzene and also the desorption of cyclohexene. However, when the catalyst was pretreated in the absence of $ZnSO_4$ under the same conditions, the pretreated catalyst gave a very poor selectivity (5.01% at 5 min) to cyclohexene. Thus based on the increase of Zn content in the pretreated catalyst, we suggests that a small part of ZnO on catalyst surface, which is difficult to react with $ZnSO_4$ in the short time of direct hydrogenation, can continue to react with $ZnSO_4$ to form the $(Zn(OH)_2)_3(ZnSO_4)(H_2O)_5$ salt in the process of pretreatment. In addition, the $(Zn(OH)_2)_3(ZnSO_4)(H_2O)_5$ salt can more stably be chemisorbed on catalyst surface after the catalyst is pretreated in the presence of $ZnSO_4$. Therefore, the pretreatment makes the catalyst exhibit the excellent selectivity to cyclohexene.

The stability of Ru–Zn(8.6%) catalyst was investigated. The catalyst was first pretreated for 22 h in the presence of $ZnSO_4$, and then the pretreated catalyst was recycled seven times without any more pretreatment and additions, and the results are listed in Fig. 8. As can be seen, the benzene conversions are stable above 50%, and the cyclohexene selectivity and yields are kept above 76% and 40% in the first six recycles respectively, indicating a good stability of the catalyst. The activity of the catalyst remarkably decreases in 7th recycle due to the inevitable catalyst loss during the recycles and six recycles without regeneration, however, the selectivity to cyclohexene and the yield are still as high as 81.4% and 26.0% respectively. Thus Ru–Zn(8.6%) catalyst has good prospects for industrial application.

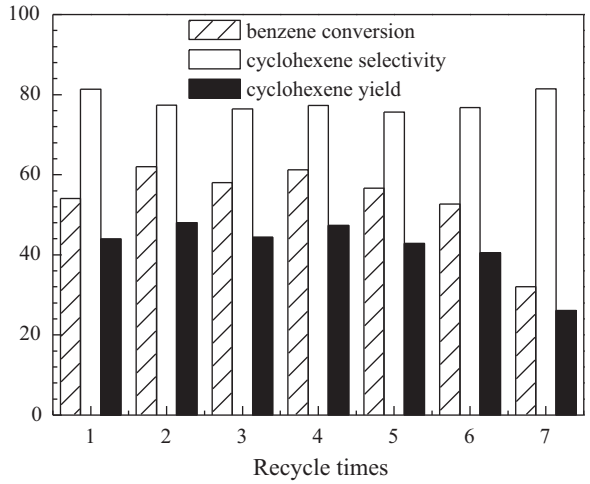

Fig. 8. Benzene conversion, cyclohexene selectivity and yields over the pretreated Ru–Zn(8.6%) catalyst in seven recycles. Pretreatment conditions: a share of catalyst, 280 ml H_2O, 49.2 g $ZnSO_4$, 5 MPa H_2, stirring rate of 800 r/min, temperature of 413 K. Reaction conditions: stirring rate of 1400 r/min, 140 ml benzene, and temperature of 423 K.

4. Conclusions

The Ru and Zn of Ru–Zn catalyst exist as metallic Ru and ZnO, and ZnO is rich on the surface. The ZnO alone cannot improve the selectivity to cyclohexene since it is difficult for it to be highly dispersed on the surface of Ru–Zn catalyst. However, the ZnO on the surface of Ru–Zn catalyst can react with the additive $ZnSO_4$ to form a insoluble $(Zn(OH)_2)_3(ZnSO_4)(H_2O)_5$ salt. The $(Zn(OH)_2)_3(ZnSO_4)(H_2O)_5$ salt can highly disperse on the surface of Ru–Zn catalyst. The $(Zn(OH)_2)_3(ZnSO_4)(H_2O)_5$ salt chemisorbed on surface of Ru–Zn catalyst plays a key role in improving the selectivity to cyclohexene. In the pretreatment, more ZnO can react with $ZnSO_4$ to form more the $(Zn(OH)_2)_3(ZnSO_4)(H_2O)_5$ salt. Moreover, the $(Zn(OH)_2)_3(ZnSO_4)(H_2O)_5$ salt can more stably be chemisorbed on catalyst surface after the catalyst is pretreated in the presence of $ZnSO_4$. Therefore, the pretreatment makes Ru–Zn(8.6%) catalyst exhibit the excellent selectivity to cyclohexene.

Acknowledgments

This work was supported by the National Nature Science Foundation of China (21273205), the Innovation Found for Technology Based Firms of China (10C26214104505) and the Scientific Research Foundation of Graduate School of Zhengzhou University. The authors thank Professor Lu Zhu for XRD analysis.

Appendix A. Supplementary data

Supplementary data associated with this article can be found, in the online version, at http://dx.doi.org/10.1016/j.apcata.2012.10.016.

References

[1] E.T. Sileiral, A.P. Umpierre, L.M. Rossi, G. Machado, J. Morais, G.V. Soares, I.J.R. Baumvol, S.R. Teixeira, P.F.P. Fichtner, J. Dupont, Chem. Eur. J. 10 (2011) 3734–3740.
[2] F. Schwab, M. Lucas, P. Claus, Angew. Chem. Int. Ed. 50 (2011) 1–5.
[3] C. Fan, Y.A. Zhu, X.G. Zhou, Z.P. Liu, Catal. Today 160 (2011) 234–241.
[4] H.J. Sun, Z.H. Chen, W. Guo, X.L. Zhou, Z.Y. Liu, S.C. Liu, Chin. J. Chem. 29 (2011) 369–373.
[5] H.J. Sun, W. Guo, X.L. Xiao, Z.H. Chen, Z.Y. Liu, S.C. Liu, Chin. J. Catal. 32 (2011) 1–9.
[6] X.L. Zhou, H.J. Sun, W. Guo, Z.Y. Liu, S.C. Liu, J. Nat. Gas Chem. 20 (2011) 53–59.
[7] F. Hartog, P. Zwietering, J. Catal. 2 (1963) 79–81.
[8] H. Nagahara, M. Ono, M. Konishi, Y. Fukuoka, Appl. Surf. Sci. 121/122 (1997) 448–451.
[9] J.M. Wu, Y.F. Yang, J.L. Chen, Chem. Ind. Eng. Prog. 22 (2003) 295–297.
[10] T. Mallat, A. Balker, Appl. Catal. A: Gen. 200 (2000) 3–22.
[11] J. Struijk, J.J.F. Scholten, Appl. Catal. A: Gen. 82 (1992) 277–287.
[12] E.V. Spinacé, J.M. Vaz, Catal. Commun. 4 (2003) 91–96.
[13] G.F. Fan, R.X. Li, X.J. Li, H. Chen, Catal. Commun. 9 (2008) 1394–1397.
[14] J. Struijk, R. Moene, T.V.D. Kamp, J.J.F. Scholten, Appl. Catal. A: Gen. 89 (1992) 77–102.
[15] J.L. Liu, Y. Zhu, J. Liu, Y. Pei, Z.H. Li, H. Li, H.X. Li, M.H. Qiao, K.N. Fan, J. Catal. 268 (2009) 100–105.
[16] L. Ronchin, L. Toniolo, Catal. Today 66 (2001) 363–369.
[17] J.W. da-Silva, A.J.G. Cobo, Appl. Catal. A: Gen. 252 (2003) 9–16.
[18] H.J. Sun, C. Zhang, P. Yuan, J.X. Li, S.C. Liu, Chin. J. Catal. 29 (2008) 441–446.
[19] S.C. Liu, Z.Y. Liu, S.H. Zhao, Y.M. Wu, Z. Wang, P. Yuan, J. Nat. Gas Chem. 15 (2006) 319–326.
[20] G.Y. Fan, W.D. Jiang, J.B. Wang, R.X. Li, H. Chen, X.J. Li, Catal. Commun. 10 (2008) 98–102.
[21] J.L. Liu, L.J. Zhu, Y. Pei, J.H. Zhuang, H. Li, H.X. Li, M.H. Qiao, K.N. Fan, Appl. Catal. A: Gen. 353 (2009) 282–287.
[22] J. Bu, J.L. Liu, X.Y. Chen, J.H. Zhuang, S.R. Yan, M.H. Qiao, H.Y. He, K.N. Fan, Catal. Commun. 9 (2008) 2612–2615.
[23] S.C. Liu, Z.Y. Liu, Z. Wang, Y.M. Wu, P. Yuan, Chem. Eng. J. 139 (2008) 157–164.
[24] S.C. Liu, Z.Y. Liu, Z. Wang, S.H. Zhao, Y.M. Wu, Appl. Catal. A: Gen. 313 (2006) 49–57.
[25] S.C. Hu, Y.W. Chen, Ind. Eng. Chem. Res. 40 (2001) 6099–6104.
[26] J.Q. Wang, Y.Z. Wang, S.H. Xie, M.H. Qiao, H.X. Li, K.N. Fan, Appl. Catal. A: Gen. 272 (2004) 29–36.
[27] P.Q. Yuan, B.Q. Wang, Y.M. Ma, H.M. He, Z.M. Cheng, W.K. Yuan, J. Mol. Catal. A: Chem. 301 (2009) 140–145.
[28] H.M. He, P.Q. Yuan, Y.M. Ma, Z.M. Cheng, W.K. Yuan, Chin. J. Catal. 30 (2009) 312–318.
[29] W. Xue, Y. Song, Y.J. Wang, D.D. Wang, F. Li, Catal. Commun. 11 (2009) 29–33.
[30] E.V. Ramos-Fernández, A.E.P. Ferreira, A. Sepúlveda-Escribano, F. Kapteijn, F. Rodríguez-Reinoso, J. Catal. 258 (2008) 52–60.
[31] J. Silvestre-Albero, J.C. Serrano-Ruiz, A. Sepúlveda-Escribano, F. Rodríguez-Reinoso, Appl. Catal. A: Gen. 292 (2005) 244–251.
[32] H. Nagahara, M. Konishi, US. Patent 4734536 (1988) (to Asahi Chem. Ind.).
[33] G. Schoen, J. Elect. Spectrosc. Relat. Phenom. 2 (1973) 75–86.
[34] M.H. Liu, J. Zhang, J.Q. Liu, W.W. Yu, J. Catal. 278 (2011) 1–7.
[35] M. Ghiaci, B. Aghabarari, A.M.B.D. Rego, A.M. Ferraria, S. Habibollahi, Appl. Catal. A: Gen. 393 (2011) 225–230.
[36] R.V. Siriwardane, J.A. Poston, Appl. Surf. Sci. 45 (1990) 131–139.
[37] I. Eo, S. Hwangbo, J. Kim, K. Hwang, Curr. Appl. Phys. 10 (2010) 1–4.
[38] Y.C. Xie, Y.X. Zhu, B.Y. Zhao, Y.Q. Tang, Stud. Surf. Sci. Catal. 118 (1998) 441–449.
[39] J. Struijk, d'Angremond, W.J.M.L. Regt, J.J.F. Scholten, Appl. Catal. A: Gen. 83 (1992) 263–295.
[40] C. Milone, G. Neri, A. Donato, M.G. Musolino, L. Mercadane, J. Catal. 159 (1996) 253–258.